21th International Conference on Renewable Energies and Power Quality (ICREPQ'23)
Madrid (Spain), 24th to 26th May 2023
Renewable Energy and Power Quality Journal (RE&PQJ)
ISSN 2172-038 X, Volume No.21, July 2023

Use of Building Façade for Active Indoor Humidity Control

K. Ghali[1], J.P. Harrouz[1] and N. Ghaddar[1]

[1] Department of Mechanical Engineering
American University of Beirut
P.O. Box 11-0236, Beirut 1107-2020, Lebanon
Phone/Fax number: +961 1 340 460, e-mail: ka04@aub.edu.lb, jeh15@mail.aub.edu, farah@aub.edu.lb

Abstract. Regulating indoor humidity levels to healthy ranges is important to provide occupants with acceptable thermal comfort and air quality conditions. Conventional techniques relied on the supply of dehumidified outdoor air to dilute the indoor generated moisture. They use vapor compression cooling either as standalone system or integrated with desiccant dehumidifiers to generate the dry air. Such systems are energy intensive and require large footprint areas, especially in hot and humid climates. This work proposes thus an energy-efficient alternative where the indoor humidity is pumped directly from the space and discharged outdoors. This system integrates a metal organic framework-based dehumidifier with the building breathable façade. The dehumidifier dries the outdoor air that is used to ventilate the façade and create the necessary driving gradient for the moisture transfer, irrespective of the outdoor air conditions. Mathematical models are developed to evaluate the system performance for an office space located in the extreme hot and humid climate of Jeddah, KSA. The proposed system resulted in 89 % and 90 % reduction in the system size and energy consumption compared to conventional systems over the peak humidity month.

Key words. Desiccant dehumidification, ventilated air gap, humidity control.

1. Introduction

With the fast-paced modernization, humans are spending longer periods in indoor spaces [1]. Providing a healthy environment within these spaces is thus crucial to protect the occupants' wellbeing. Such environments are created by maintaining indoor generated species such water vapor, CO_2, and VOCs to ensure good air quality. Among these species, careful consideration should be given to the indoor H_2O levels [2]. In fact, high relative humidity (RH) levels cause building dampness, which triggers asthmatic reactions [3]. Moreover. high RH increase the risk of virus transmission and affect the perceived thermal comfort by the occupants [4]. On the other hand, low indoor RH levels cause skin dryness and eye irritation [5]. It is therefore important to control indoor humidity levels, which is conventionally carried out by pumping dehumidified air into the space to dilute the indoor-generated moisture [6]. Such techniques rely on the use of vapor compression cooling either as standalone systems or integrated with desiccant dehumidifiers to generate this dried air. These methods are known to be energy intensive, especially in hot and humid climates, hence the need for more energy-efficient RH control methods.

Recent efforts are made to directly remove the indoor moisture using hygroscopic materials such as cloth cotton curtains [7], and metal organic framework (MOFs) desiccant wall panel [8]. These materials act as moisture buffers and can reduce the fluctuations in indoor RH levels. However, they suffered from limited capacity and a batch operation that requires complex switching mechanism [9]. Another approach for direct humidity control would be to exploit the building structure to drive the humidity outdoors [10]. Building structures have always been exploited to reduce the sensible cooling loads of indoor spaces by incorporating ventilated facades [11]. However, most building façades are of a breathable nature, which facilitates moisture transfer. Hence, their use can be expanded to reduce the building latent load. This technique relies thus on the gradient in the water vapor pressure between the indoor and outdoor air as driver for the moisture flow. Accordingly, this approach has been applied only to dry climates to avoid the reversal of the moisture flow from outdoor environment to the indoor space. Nevertheless, its applicability has been expanded to humid regions by pumping dry air into the building structure [12]. Such system used a rotating bed packed with MOFs based desiccant to dehumidify the outdoor air and supply it the building façade. This created the needed driving gradient for the moisture transfer from the indoor space, irrespective of the outdoor air conditions. Accordingly, the ventilated façade can actively control the indoor humidity levels. The performance of this system has been evaluated under the moderate humid climate of Beirut and showed a reduction of 66 % reduction in the system cost and 86 % in its operating cost. Nonetheless, it is important to study the performance of this system under extreme weather conditions to determine its range of applicability. For this reason, mathematical models are developed for the heat and mass transfer of the desiccant dehumidifier and the ventilated façade. The models are used to design and operate the system for an office space during the peak humidity conditions of Jeddah, KSA. The system size and energy consumption are then compared to conventional systems employing vapor compression cooling integrated with MOFs-based dehumidifiers. This is important to determine the impact of the proposed system on the building's energy bill.

2. System description

The proposed system is implemented in an office space located in a hot and humid climate. To ensure thermal comfort, the space air temperature is maintained at 24 °C using a vapor compression cooling system that is capable of only sensible cooling. Outdoor air flowrate is introduced into the space to meet the air quality requirements. Accordingly, CO_2 is chosen as the surrogate gas to determine the outdoor air flowrate needed to meet the ASHRAE level of 1000 ppm. Finally, the space relative humidity levels are maintained at 60 % using the proposed system that consists of three main components as shown in Fig. 1(a): a rotating packed bed, a breathable ventilated façade, and an air-to-air heat exchanger. The rotating packed bed employ MOFs-based desiccant to dehumidify the outdoor air. The building façade consist of an airgap whose indoor side is formed of a breathable insulation. The latter enable the reduction of the sensible heat gain into the space from the hot dried outdoor air without hindering moisture transfer. The air-to-air heat exchanger is used to cool the dried outdoor air before it is introduced into the façade to reduce the sensible heat gains to the space.

The system operation is thus summarised as follows: the outdoor air at flowrate ($\dot{m}_{fa}$) at state (1) enters the desiccant dehumidifier. The resulting hot and dry air at state (2) is cooled with the outdoor air in the heat exchanger to state (3) before it is introduced in the airgap. The dry air picks up the moisture transferred from the indoor space before it is discharged to the outdoors at state (4). Simultaneously, the outdoor air at a flowrate of ($\dot{m}_{pa}$) is used to regenerate the desiccant. It is thus preheated in the heat exchanger from state (1) to state (2') before it enters the external heater to reach the regeneration temperature (T_{reg}) at state (3'). The regeneration airflow is then discharged to the outdoor at state (4') with the purged water vapor. The different air states are shown on the psychrometric chart of Fig. 1(b). Note that a third stream of outdoor air at a flowrate of ($\dot{m}_{oa}$) is mixed with the room return air before they are cooled to the required supply temperature (T_{sup}) and pumped into the space at a flowrate of ($\dot{m}_{sa}$) to meet the required temperature and CO_2 levels in the office.

For this system, the desiccant dehumidifier is packed with MIL-101-Cr beads, which is a MOFs desiccant characterized by its high water capacity and fast kinetics [13]. This desiccant showed an uptake capacity that reached 1.2 kg/kg for water vapor with a regeneration temperature of 60 °C [14]. Moreover, the rotating packed bed cross section is divided into two main sections: the dehumidification and regeneration sections with a ratio of 3:1. This is due to the higher kinetics of desorption, which allows the reduction of the regeneration region (regeneration time) [15]. In addition, mineral wool is used as insulator due to its low water vapor diffusion resistance [16].

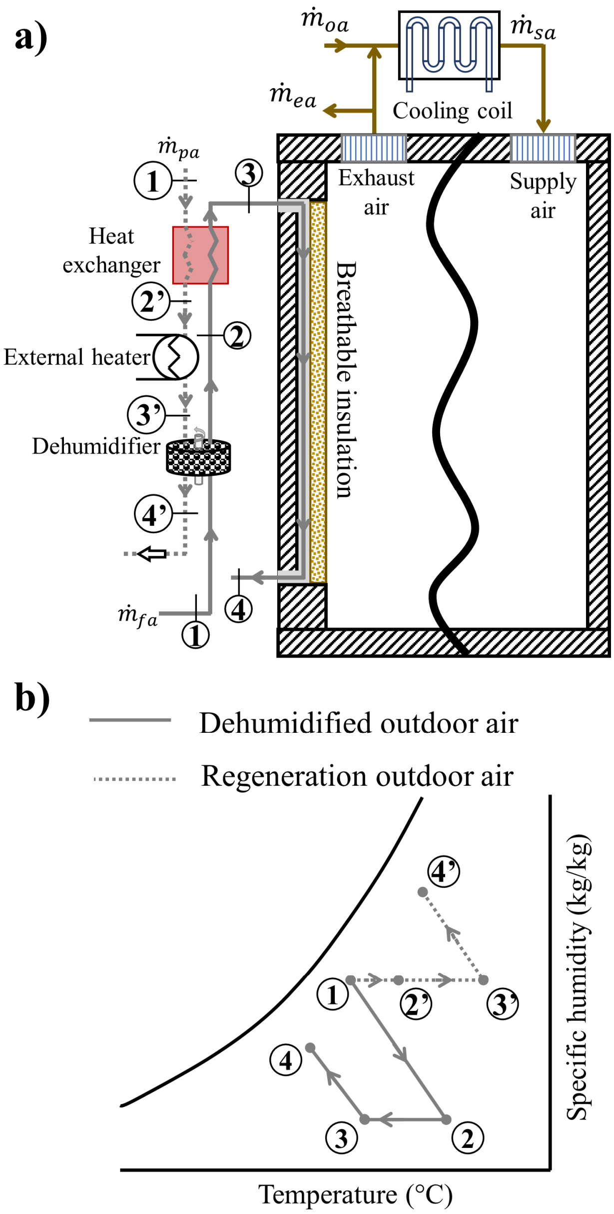

Fig. 1. Schematic of a) proposed system and b) psychrometric chart of the process outdoor air flowrates.

3. Methodology

Mathematical models are developed for the heat and mass transfer in the airgap of the ventilated façade and in the desiccant dehumidifier. The models are used to size and optimize the system operation to meet the required indoor moisture levels.

A. *Ventilated air gap*

The air in the ventilated façade exchange both heat and water vapor with the indoor air through the breathable insulation. Since the used mineral wool insulation has a negligible water vapor uptake, a steady one-dimensional couple heat and mass transfer model is adopted [17]. The resulting energy and mass balances for the airgap are given by the equivalent resistance scheme:

$$\frac{dT_{oa}}{dz} = \frac{U_H A_{ins}}{\dot{m}_{oa} c_{p,oa}} \left(1 + \frac{c_{p,wv}}{c_{p,oa}} (\omega_{ia} - \omega_{oa})\right) (T_{ia} - T_{oa}) \quad (1)$$

$$\frac{d\omega_{oa}}{dz} = \frac{U_M A_{ins}}{\dot{m}_{oa}} (\omega_{ia} - \omega_{oa}) \quad (2)$$

where $\bar{z}$ (-) is the normalized space coordinate along the channel height H_{oa} (m). T_{oa} (K), T_{ia} (K), ω_{oa} (kg/kg) and ω_{ia} (kg/kg) are the outdoor and indoor air temperatures and specific humidity, respectively. $C_{p,oa}$ (J/kg·K) and $C_{p,wv}$ (J/kg·K) are the specific heat capacity of outdoor air and water vapor respectively. A_{ins} (m^2) is the insulation layer area, U_H (W/m^2·K) and U_M (kg/m^2·s) are the overall heat and mass transfer coefficients, respectively.

B. Desiccant dehumidifier

The rotating and fixed packed beds share similarity in terms of desiccant configuration and airflow patterns. Moreover, the low rotational speed of the rotating packed bed, radial air convection can be neglected [18]. Hence, a transient one-dimensional coupled heat and mass transfer between the airflow and the desiccant. The water vapor mass balance for the air stream is thus given by

$$\varepsilon_g \rho_{oa} \frac{\partial \omega_{oa}}{\partial t} + \rho_{oa} u_{oa} \frac{\partial \omega_{oa}}{\partial y} - D_{v,s} \frac{\partial^2 \omega_{oa}}{\partial y^2} + (1 - \varepsilon_g)\rho_s \frac{\partial \bar{q}_s}{\partial t} = 0 \quad (3)$$

where ε_g (-) is the dehumidifier total porosity, ρ_{oa} (kg/m^3) is the outdoor air density, u_{oa} (m/s) is the air velocity, $D_{v,s}$ (m^2/s) is the water vapor diffusivity, ρ_s (kg/m^3) is the desiccant density and $\frac{\partial \bar{q}_s}{\partial t}$ (kg/kg·s) is the adsorption rate. For the solid side mass transfer, the linear driving force (LDF) model is adopted where the film, micro- and macropore mass transfer resistances are lumped into a single term, the LDF time constant k_{LDF} (s^{-1}). The water vapor mass balance is given by

$$\frac{\partial \bar{q}_s}{\partial t} = k_{LDF} (\bar{q}^*_s - \bar{q}_s) \quad (4)$$

where $\bar{q}^*_s$ (kg/kg) and $\bar{q}_s$ (kg/kg) are the equilibrium and actual uptake of the desiccant. The detailed model is presented by Harrouz et al. [19] and not reported here for conciseness.

C. Numerical solution

The different models are integrated in a MATLAB code where the different heat and mass balances are solved using the finite volume approach with implicit first order upwind scheme. A time step independence test yielded a time step of 10^{-5} s that is adopted to ensure accurate results with acceptable computational time. The convergence criterion is met when the difference between two different iteration is lower than the tolerance of 10^{-8} for all the calculated parameters.

4. Case Study

The system performance is evaluated for a case study of a typical four-workers office space of (5 m × 5 m × 3 m) located in Jeddah on the coastal region of KSA facing the Red Sea. The prevailing weather in this location is characterized by extreme hot and humid conditions where peak outdoor air dry bulb and dew point temperatures reach 41 °C and 28.8 °C, respectively. The office envelope and occupancy schedule properties are provided by Katramiz et al. [20]. The generation rate of water vapor and CO_2 are set to 11.57 mg/(s·person) and 10.8 mg/(s·person) [21].

The proposed system is installed on one of the office façades and its area is fixed at 50 % of the wall area [8], with a height of 2 m while the airgap is set to 2 cm [22]. To ensure an effective mass transfer, the air velocity is set to 1.5 m/s, which results in a flowrate of 0.14 kg/s. The rotating packed bed is sized to hold the maximum amount of water to be removed from outdoor air flowrate $\dot{m}_{fa}$ during peak humidity conditions corresponding to 25.4 g/kg. On the other hand, the outlet air humidity from the dehumidifier is set to 7 g/kg create the necessary gradient with the indoor air at 11.3 g/kg. by fixing the cycle time at 1200 s, which is equivalent to 3 RPH rotational speed [15].

For the conventional system, the same inlet conditions and cycle time are adopted for the dehumidifier design, however, the outlet humidity is set to 9 g/kg, necessary to dilute the generated indoor moisture. The dehumidifier is designed to remove the peak latent load which occur during the peak humidity month of August.

Having these conditions, the needed adsorbent mass to remove the latent load in the proposed and conventional systems are 2.5 kg and 20 kg, respectively. The corresponding bed diameter and length are 0.35 m and 0.15 m for the proposed system while for the conventional system, they are set to 0.7 m and 0.25 m, respectively. Accordingly, an initial saving of 89 % was achieved using the proposed system.

5. Results and discussion

The developed mathematical models were validated by Harrouz et al. [12] for different air conditions in the airgap and the maximum discrepancies were less than 10 % for all calculated parameters of both the ventilated airgap and desiccant dehumidifier models.

The validated models were then used to properly operate the proposed system. For this reason, the outdoor air flowrates $\dot{m}_{fa}$ and $\dot{m}_{sa}$ entering the dehumidifier in both proposed and conventional systems were determined to maintain the indoor air conditions specified in Section 2 during the peak humidity month of August as shown in Fig. 2(a). The corresponding electrical energy for the fan operation ($E_{e,f}$), vapor compression cooling coil ($E_{e,c}$) as well as the regeneration thermal energy (E_t) are shown in Fig. 2(b-c).

The dehumidified outdoor air flowrate in the proposed system ($\dot{m}_{fa}$) varied with the outdoor air specific humidity. It increased from 0.11 kg/s around noon hours where the outdoor humidity was at the lowest values of 22.8 g/kg and reached 0.14 kg/s at peak humidity of 25.4 g/kg (Fig. 1(a)). On the other hand, the dehumidified outdoor air in the conventional system consisted of the space supply flowrate ($\dot{m}_{sa}$). Accordingly, this flowrate was dictated by the space cooling load and followed its hourly variation pattern. It increased from 0.85 kg/s during early hours of the day when the outdoor conditions of temperature and radiation were low and reached 1.82 kg/s at 16:00 hr at the peak load hour (Fig. 1(a)).

The proposed system operation required thermal energy that varied between 0.49 kWh and 0.7 kWh fan electrical energy between 0.31 kWh and 0.6 kWh and coil electrical energy between 2.1 kWh and 3.85 kWh (Fig. 2(b)). The first two parameters followed the pattern of $\dot{m}_{fa}$ whereas the last one followed the cooling load of the office space. On the other hand, the thermal and electrical energy consumption of the conventional system was higher by two orders of magnitude. They varied between 3.3 kWh and 7 kWh for E_t and 5.9 kWh and 50.6 kWh for $E_{e,f}$ (Fig. 2(c)). This was due to the relatively higher outdoor air flowrate treated in the dehumidifier that necessitated higher thermal energy for regeneration and high electrical energy to drive the fan. On the other hand, the electrical energy needed for the cooling coil varied within the same order of magnitude and increased from 3.4 kWh to 7 kWh with the increase in the space load. The highest reduction was achieved at the level of the fan electrical energy, which reached 98 %. On the other hand, the proposed system achieved a reduction of 89.5 % in the thermal energy and 42 % reduction in the cooling coil energy. Assuming an electricity cost of 0.13 USD/kWh and a thermal energy cost of 0.019 USD/kWh, the proposed system resulted in a reduction of 90 % in the operating cost of the office space humidity control system compared to the conventional system during the peak humidity month.

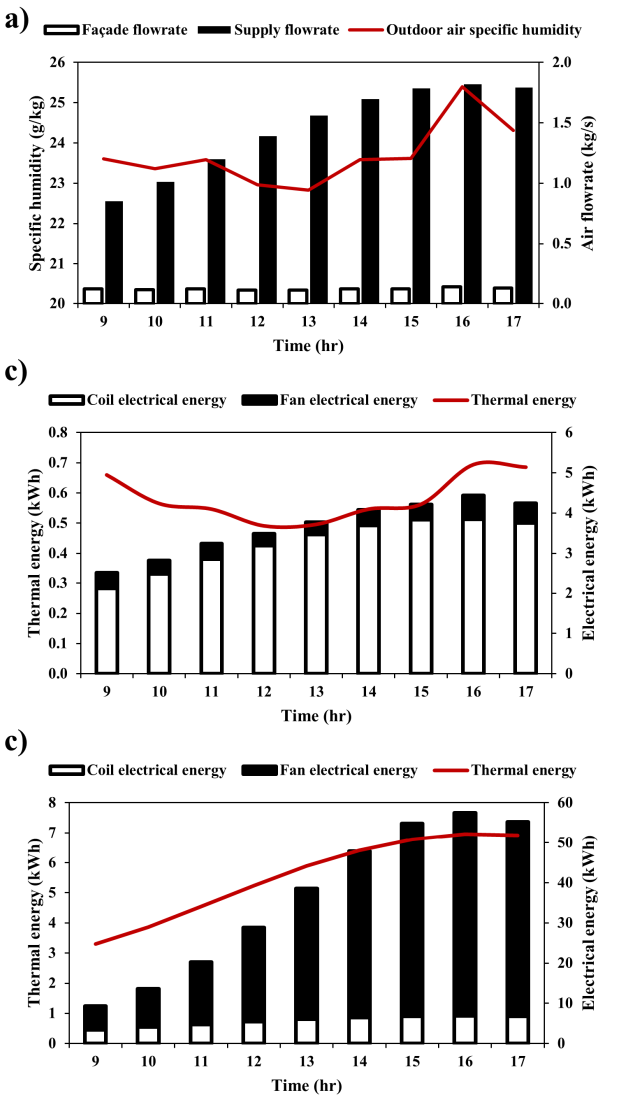

Fig. 2. The obtained a) outdoor air flowrate entering the dehumidifier and the corresponding thermal and electrical energy consumption for b) the proposed and c) conventional systems.

6. Conclusion

In this work, a ventilated façade is proposed to actively control indoor humidity levels through direct removal of the generated moisture in enclosed spaces. The system uses a MOFs based desiccant dehumidifier to generate dry air that is used to ventilate the building façade, creating a humidity gradient to drive the indoor moisture outdoors. Mathematical models were developed for the heat and mass balances for the different subcomponents. The models are used to size and operate the proper system to meet the required indoor humidity levels for a case study of a typical office located in the extreme humid climate of Jeddah, KSA. Over the peak humidity month of August, the proposed system reduced by 89 % and 90 % the system size and operating cost, respectively, compared to the conventional system employing vapor compression cooling integrated with desiccant dehumidifier. This indicates that as the outdoor humidity increased, the savings obtained by the proposed system increased as well.

Acknowledgment

The authors would like to acknowledge the financial support of the American University of Beirut – Masri Institute of Energy and Natural Resources. The findings achieved herein are solely the responsibility of the authors.

References

[1] N. E. Klepeis *et al.*, "The National Human Activity Pattern Survey (NHAPS): a resource for assessing exposure to environmental pollutants," *Journal of Exposure Science & Environmental Epidemiology*, vol. 11, no. 3, pp. 231-252, 2001.

[2] S. H. Subedi, "A Mathematical Study of Effect of Humidity on Human Skin Temperature at Warm Environment," *Journal of the Institute of Engineering*, vol. 16, no. 1, pp. 141-150, 2021.

[3] E. Heseltine and J. Rosen, "WHO guidelines for indoor air quality: dampness and mould," 2009.

[4] A. Aganovic, Y. Bi, G. Cao, F. Drangsholt, J. Kurnitski, and P. Wargocki, "Estimating the impact of indoor relative humidity on SARS-CoV-2 airborne transmission risk using a new modification of the Wells-Riley model," *Building and environment*, vol. 205, p. 108278, 2021.

[5] A. Baughman and E. A. Arens, "Indoor humidity and human health--Part I: Literature review of health effects of humidity-influenced indoor pollutants," *ASHRAE transactions*, vol. 102, pp. 192-211, 1996.

[6] M. Shehadi, "Review of humidity control technologies in buildings," *Journal of Building Engineering*, vol. 19, pp. 539-551, 2018.

[7] S. Salloum, K. Ghali, and N. Ghaddar, "Moisture buffering capacity of novel solar□regenerated rotating hygroscopic curtain system," *International Journal of Energy Research*, vol. 39, no. 14, pp. 1942-1953, 2015.

[8] X. Feng, M. Qin, S. Cui, and C. Rode, "Metal-organic framework MIL-100 (Fe) as a novel moisture buffer material for energy-efficient indoor humidity control," *Building and Environment,* vol. 145, pp. 234-242, 2018.
[9] Y. Zhang, L. Wu, X. Wang, J. Yu, and B. Ding, "Super hygroscopic nanofibrous membrane-based moisture pump for solar-driven indoor dehumidification," *Nature communications,* vol. 11, no. 1, pp. 1-11, 2020.
[10] M. Nizovtsev, V. Letushko, V. Y. Borodulin, and A. Sterlyagov, "Experimental studies of the thermo and humidity state of a new building facade insulation system based on panels with ventilated channels," *Energy and Buildings,* vol. 206, p. 109607, 2020.
[11] A. De Gracia, A. Castell, L. Navarro, E. Oró, and L. F. Cabeza, "Numerical modelling of ventilated facades: A review," *Renewable and Sustainable Energy Reviews,* vol. 22, pp. 539-549, 2013.
[12] J. P. Harrouz, K. Ghali, M. Hmadeh, R. Slim, E. Katramiz, and N. Ghaddar, "Design and control of MOFs-based indoor humidity pump integrated into the building's ventilated façade in hot and humid climates," *Energy Conversion and Management,* vol. 268, p. 115983, 2022.
[13] E. Elsayed, P. Anderson, A.-D. Raya, S. Mahmoud, and A. Elsayed, "MIL-101 (Cr)/calcium chloride composites for enhanced adsorption cooling and water desalination," *Journal of Solid State Chemistry,* vol. 277, pp. 123-132, 2019.
[14] H. W. B. Teo, A. Chakraborty, and S. Kayal, "Post synthetic modification of MIL-101 (Cr) for S-shaped isotherms and fast kinetics with water adsorption," *Applied Thermal Engineering,* vol. 120, pp. 453-462, 2017.
[15] C. Ruivo, J. Costa, A. Figueiredo, and A. Kodama, "Effectiveness parameters for the prediction of the global performance of desiccant wheels–an assessment based on experimental data," *Renewable energy,* vol. 38, no. 1, pp. 181-187, 2012.
[16] M. Jiřičková and R. Černý, "Effect of hydrophilic admixtures on moisture and heat transport and storage parameters of mineral wool," *Construction and Building Materials,* vol. 20, no. 6, pp. 425-434, 2006.
[17] F. Abdollahi, S. Hashemifard, A. Khosravi, and T. Matsuura, "Heat and mass transfer modeling of an energy efficient Hybrid Membrane-Based Air Conditioning System for humid climates," *Journal of Membrane Science,* vol. 625, p. 119179, 2021.
[18] K. S. Hwang and W. K. Lee, "The adsorption and desorption breakthrough behavior of carbon monoxide and carbon dioxide on activated carbon. Effect of total pressure and pressure-dependent mass transfer coefficients," *Separation science and technology,* vol. 29, no. 14, pp. 1857-1891, 1994.
[19] J. P. Harrouz, E. Katramiz, K. Ghali, D. Ouahrani, and N. Ghaddar, "Comparative analysis of sustainable desiccant–Evaporative based ventilation systems for a typical Qatari poultry house," *Energy Conversion and Management,* vol. 245, p. 114556, 2021.
[20] E. Katramiz, N. Ghaddar, and K. Ghali, "Daytime radiative cooling: To what extent it enhances office cooling system performance in comparison to night cooling in semi-arid climate?," *Journal of Building Engineering,* vol. 28, p. 101020, 2020.
[21] J. P. Harrouz, K. Ghali, M. Hmadeh, N. Ghaddar, and S. Ghani, "Feasibility of MOF-based carbon capture from indoor spaces as air revitalization system," *Energy and Buildings,* vol. 255, p. 111666, 2022.
[22] T. Zhang and H. Yang, "Optimal thickness determination of insulating air layers in building envelopes," *Energy Procedia,* vol. 152, pp. 444-449, 2018.